Since January 2020 Elsevier has created a COVID-19 resource centre with free information in English and Mandarin on the novel coronavirus COVID-19. The COVID-19 resource centre is hosted on Elsevier Connect, the company's public news and information website.

Energy & Buildings 240 (2021) 110883

Contents lists available at ScienceDirect

Energy & Buildings

journal homepage: www.elsevier.com/locate/enb

Occupant-density-detection based energy efficient ventilation system: Prevention of infection transmission

Junqi Wang [a,b,c], Jingjing Huang [c], Zhuangbo Feng [a], Shi-Jie Cao [a,d,*], Fariborz Haghighat [e]

[a] School of Architecture, Southeast University, 2 Sipailou, Nanjing 210096, China
[b] School of Environmental Science and Engineering, Suzhou University of Science and Technology, Suzhou 215009, China
[c] Jiangsu Key Laboratory of Intelligent Building Energy Efficiency, Suzhou, Jiangsu 215009, China
[d] Global Centre for Clean Air Research, Department of Civil and Environmental Engineering, Faculty of Engineering and Physical Sciences, University of Surrey, United Kingdom
[e] Energy and Environment Group, Department of Building, Civil and Environmental Engineering, Concordia University, Montreal H3G 1M8, Canada

ARTICLE INFO

Article history:
Received 22 January 2021
Revised 16 February 2021
Accepted 1 March 2021
Available online 9 March 2021

Keywords:
Ventilation
COVID-19
Infection risk
Occupant detection
Energy conservation
Public buildings

ABSTRACT

Ventilation plays an important role in prevention and control of COVID-19 in enclosed indoor environment and specially in high-occupant-density indoor environments (e.g., underground space buildings, conference room, etc.). Thus, higher ventilation rates are recommended to minimize the infection transmission probability, but this may result in higher energy consumption and cost. This paper proposes a smart low-cost ventilation control strategy based on occupant-density-detection algorithm with consideration of both infection prevention and energy efficiency. The ventilation rate can be automatically adjusted between the demand-controlled mode and anti-infection mode with a self-developed low-cost hardware prototype. YOLO (You Only Look Once) algorithm was applied for occupancy detection based on video frames from surveillance cameras. Case studies show that, compared with a traditional ventilation mode (with 15% fixed fresh air ratio), the proposed ventilation control strategy can achieve 11.7% energy saving while lowering the infection probability to 2%. The developed ventilation control strategy provides a feasible and promising solution to prevent transmission of infection diseases (e.g., COVID-19) in public and private buildings, and also help to achieve a healthy yet sustainable indoor environment.

1. Introduction

COVID-19 is a respiratory disease caused by a coronavirus (SARS-COV-2), which has a high-level of infection and morbidity [1,2]. Till 14 February 2021, COVID-19 has caused 108 million confirmed infected cases including 2.38 million deaths [3]. As the reopening of social economy, there is a high probability to involve large number of transportation activities, and creating large mobility of people. Thus, there is a strong need to develop control strategies to prevent the transmission of COVID-19 and alike diseases in public and private buildings (PPBs) (e.g., airport terminal, train station, bus station, super market and shopping centers, universities, entertainment events, etc.). For this purpose, some control measures have been widely used [1,4], such as the source control (to separate suspected infected patients), virus spread control (to restrict going out), virus tracing, etc.

In PPBs, ventilation can play essential and important role in reducing the infection transmission. It introduces outdoor air to dilute the indoor air contaminants generated by the occupants and their activities. ASHRAE Standard 62.1 [5] and Chinese Standard [6] specify the minimum amount of outdoor air that is to be provided by the HVAC systems. This airflow rate is calculated based on maximum occupancy conditions. The PPBs have highly transient occupancy condition, hence could provide fertile ground for transmission and infection during high-occupancy periods, and over ventilation during low-occupancy periods (which is a waste of energy).

The transmission of SARS-CoV-2 mainly include contact transmission, exhaled droplet transmission and aerosol transmission [2,7,8]. The exhaled droplets of infectors may fall down and contaminate the surface, which could be infective for few hours to few days [9,10]. Besides, the virus could re-enter the air upon the surface disturbances [11]. To reduce the infection risk of contact transmission, frequent hand washing with sanitize and surface disinfection are important; for contact and exhaled droplet transmission, wearing masks and keeping social distance are normally

* Corresponding author at: School of Architecture, Southeast University, 2 Sipailou, Nanjing 210096, China.
E-mail address: shijie_cao@seu.edu.cn (S.-J. Cao).

https://doi.org/10.1016/j.enbuild.2021.110883
0378-7788/

recommended [1,12]. However, there are common occasions of dense crowd (e.g., queueing for boarding, for purchasing in supermarket, or for security checking) and off-mask activities (e.g., drinking or dining) in PPBs (see Fig. 1), which could pose a potential risk of infection especially when people exposed to a dense and crowded environment. The ventilation system is thus an efficient and important approach to reduce the transmission of infection in PPBs: the system introduces the outdoor air to dilute the indoor air contaminant that is mainly responsible for the aerosol transmission [1].

When the situation of dense crowd occurs, ventilation rate should be increased to reduce the infection risk. However, the standard minimum outdoor airflow rate of public buildings is insufficient to control the infection risk at low level (e.g., 2%) [15]. It is thus essential and widely recommended to improve the ventilation rate for the sake of reducing infection probability (IP) of COVID-19 in such high-density indoor environment [2]. For instance, it is reported that to control the IP in office under 2%, the ventilation rate should be improved from 30 $m^3/(h{\cdot}p)$ (a designed rate) to 225 $m^3/(h{\cdot}p)$ for a full occupant density with a 2-h exposure time [15]. However, high ventilation rates would result in higher energy consumption and may cause some thermal discomfort [15]. Especially for PPBs, which may have variable temporal distribution and uneven spatial distribution of occupants [16]. Under this circumstance, the ventilation rate can be reduced to a lower level in order to save energy [17]. Therefore, the challenge is how to balance the ventilation energy consumption and the prevention of infection risk in such indoor environment during pandemic [7]. One technique to reduce this transmission is demand-controlled ventilation (DCV) systems [18]. This approach gives the ability to control the supply of outdoor airflow rate based on the building occupant density.

It is however, challenging and expensive to re-design and retrofit the existing ventilation system [19–21]. Hence, a more practical solution is probably to make some minor adjustments or improvement to the existing ventilation system using the concept of DCV. This can be achieved by making the existing ventilation system capable of dynamically monitoring occupant density and adjusting the ventilation rate. Hereby, the efficient detection of occupant density is of great importance [22]. Currently, the occupant detection is based on environmental monitoring [23], information and communication technology (e.g. Wi-Fi) [24,25] and visual information using cameras [26–28]. Among the three occupant detection methods, the camera-based method is recommended since it cannot only provide the number and location of occupants, but also monitor the crowd gathering and individual behaviors (like hand shaking and hugging) as well as the occupant tracking [29]. Moreover, surveillance cameras are normally used in PPBs for the security and safety purposes. The information collected by these cameras can be easily provided to the ventilation system (almost at no extra cost on the hardware of sensing).

In combating the COVID-19, many deep-learning-powered camera-based methods have been developed and used for social distance detection and face mask detection [30–32]. This manuscript proposes a methodology based on reducing the transmission of infection diseases in high density public buildings by applying the occupant-related information collected from existing cameras to control the ventilation rate. With this idea, many interesting and important issues are worthwhile to be investigated for an integrated camera-based ventilation control solution including the deep-learning method for occupant detection, infection risk evaluation as well as building energy efficiency etc.

2. Methodology

2.1. Research overview

Fig. 2 shows the schematic of the proposed ventilation control system. First, based on the video captured by the camera, the occupants are detected by YOLO (You Only Look Once) algorithm (detailed in Section 2.2.1), and it provides the bounding box for the detected occupant. Then, the location of the detected occupant is determined according to coordinates of the bounding box (detailed in Section 2.2.2). With this information, the sub-zonal occupant density is obtained (i.e. the sub-zonal occupant number divided by the area of the zone), which can be used to determine the ventilation mode (DCV mode or anti-infection mode) by comparing it with a pre-set threshold ("θ"), corresponding to the recommended safe social distance, i.e., 2 m [33,34].

If the sub-zonal occupant density is lower than or equal to θ, the demand-controlled mode is activated and the ventilation rate is determined according to the Standard (e.g., [6]); If the sub-zonal occupant density is higher than θ, the signal is sent to the corresponding management personnel. Meanwhile, the anti-infection mode of ventilation is activated and the ventilation rate is adjusted based on the occupant density (based on the calculation using Wells-Riley model) to lower down the IP below a targeted value. Wells-Riley model is selected considering that it is has been widely used for the infection risk evaluation [35,36]. Finally, the IP and ventilation energy consumption are evaluated (corresponding to the ventilation rate).

Fig. 1. (a) An airport in disarray over screening (from BBC news [13]); (b) Queueing in a metro station [14]

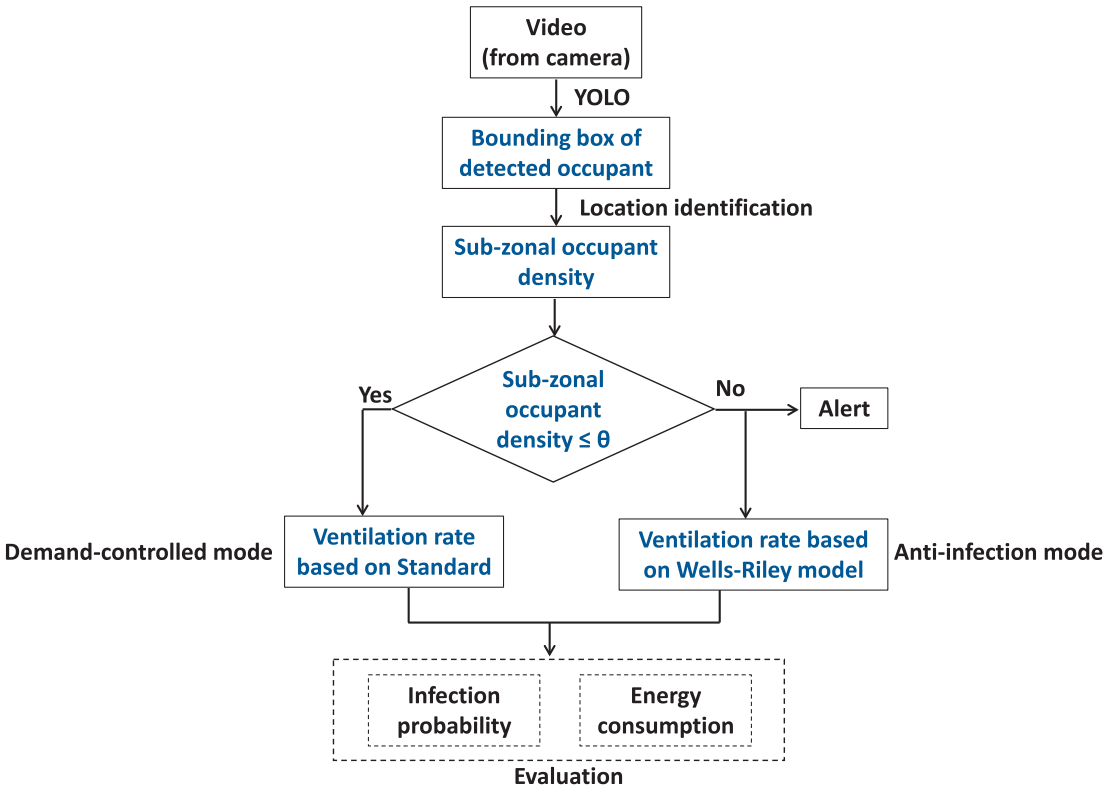

Fig. 2. Research diagram of the proposed ventilation control.

2.2. Method description

2.2.1. YOLO (You only Look Once) algorithm for occupant detection

Redmon et al. [37] proposed the YOLO algorithm which pioneered the solution in deep-learning based object detection and it has been applied in many areas, such as transportation [38], robotics [39], and safety management [40]. YOLO version 4 is selected in this study since it performed faster and more accurate than most modern object detection algorithms [41].

Fig. 3 shows the schematic of the system. Firstly, the input video frame is adjusted to a unified length and width, and then, the frame is fed into the convolutional network (a class of deep neural networks that commonly applied in visual information processing) to predict bounding boxes and the associated confidence scores. Next, the optimal bounding box of each detected object is identified through the non-maximum suppression [37]. With the information of bounding boxes, the detected occupant and its position can be obtained (detailed in the next section).

2.2.2. Location identification of detected occupant

The video obtained from online monitoring of camera is composed of a number of sequential frames (pictures) (see Fig. 4 (a)). The YOLO algorithm generates a bounding box for the detected occupant. To determine the occupant location in sub-zone level, boundary curves are defined (see in Fig. 4) based on the sub-zones corresponding to the ventilation diffusers (sub-zones can be divided by the serving area of ventilation diffusers [6,42]). The occupant location is determined by using the bottom center of bounding box which represents the standing location of the occupant. The origin of coordinates is set at the left upper corner in the video frame (see Fig. 4 (b)). Based on the coordinate equations of boundary curves and the coordinates of the bottom center of bounding box, the occupant location (sub-zone belonging) can be identified. To obtain the coordinate equations of the boundary curves, a MATLAB code (see Appendix C) was developed to get the coordinates of the sample points on the boundary. Since the boundary curves (See Fig. 4) are close to a quadratic shape, a quad-

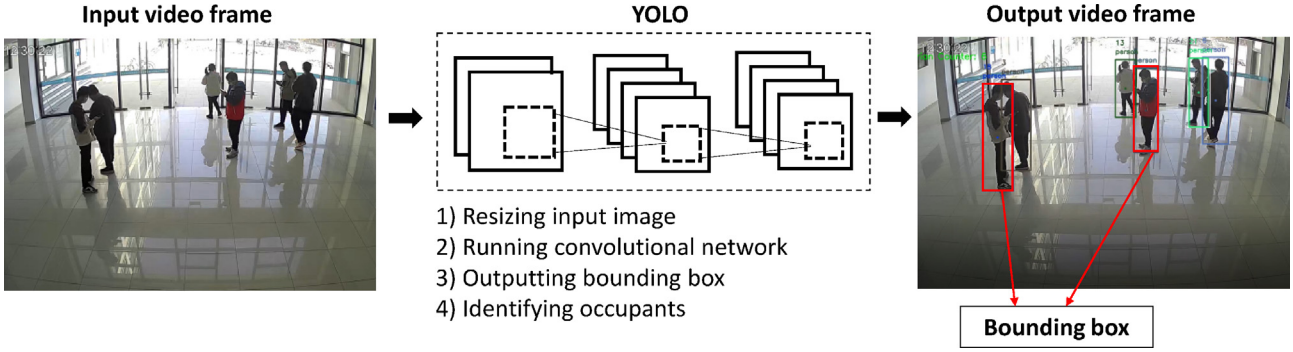

Fig. 3. Detection process of YOLO algorithm.

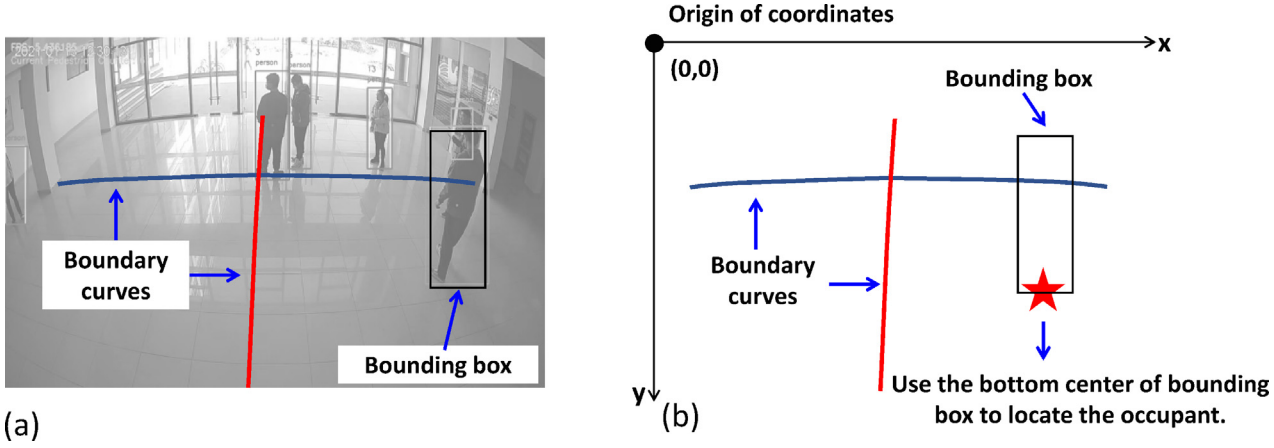

Fig. 4. (a) boundary curves and bounding box; (b) illustration of location identification.

ratic equation is assumed and the coordinate equations of the boundaries are obtained by curve fitting.

2.2.3. Ventilation strategies

DCV mode

Based on the detected sub-zonal occupant density, the amount of outdoor air can be determined and adjusted based on the design Standard. For instance, the Chinese Standard classifies the occupant density (P_F) into three levels for the waiting room of public transportation buildings (refer to Table 1) [6]. With the variation of occupant density levels, the corresponding minimal ventilation rates can be recommended (see Table 1), i.e., 15, 16 to 19 $m^3/(h{\cdot}p)$.

Anti-infection ventilation mode

The anti-infection mode of ventilation targets for controlling an IP below a certain target (e.g., IP $\leq$ 2%). Based on the Wells-Riley model (see Equation (1), Section 2.4), the required ventilation rate can be calculated. The infection risk can be calculated using a modified Wells-Riley model which includes the effects of social distance and ventilation effectiveness [15],

$$IP = 1 - exp(-P_d \frac{Bqpt}{E_z Q/N}) \quad (1)$$

$$P_d = (-18.19 \ln(d) + 43.276)/100 \quad (2)$$

where IP is the infection probability, P_d is the social distance index, B is initial infection rate, q is the quantum generation rate produced by one infector (quantum/s), p is the pulmonary ventilation rate of susceptible individual (m^3/s), t is the exposure time (s), E_z is the air distribution effectiveness (see [5]), Q is the room ventilation rate (m^3/s), N is the number of occupants, and d is the transmission distance (m).

2.2.4. Ventilation system energy consumption

The ventilation system energy consumption includes both the energy consumption of the air-conditioning system and the fan. The energy consumption of conditioning the outdoor air (by the air-handling unit) can be estimated by equation (3), where the Q_{fresh} is calculated based on the enthalpy difference (between the indoor air and outdoor air) and the airflow rate.

$$P_{fresh} = Q_{fresh}/COP \quad (3)$$

where P_{fresh} is the energy consumption of conditioning the outdoor air (W), Q_{fresh} is the ventilation load (W), COP is the coefficient of performance. The power of fans is estimated by the affinity law (equation (4)),

$$P_{fan} = \beta F^3 \quad (4)$$

where P_{fan} is the power consumption of fan (kW), F is the airflow rate (m^3/s), and β is the coefficient (β is set to 0.8 based on the catalog of a fan).

Table 1
Flow rate of fresh air ($m^3/(h{\cdot}p)$) based on Standard [6]

Building type	Occupant density P_F (p/m^2)[#]		
	$P_F \leq 0.4$	$0.4 < P_F \leq 1.0$	$P_F > 1.0$
waiting room of public transportation buildings	19	16	15

[#] : p/m^2 stands for people per square meter.

2.3. Case study

2.3.1. Procedure

To demonstrate the proposed method, a schematic indoor space of a PPB is presented in Fig. 5. Ventilation is designed with four supply air diffusers mounted at the room ceiling and two outlets along the side walls, which is a typical design considering its easy installation and well-functioning airflow pattern. For the easy design and understanding, each diffuser is used to ventilate a corresponding sub-zone (four equal-area sub-zones). As it has been reported, airflow pattern plays an essential role in air pollutant (i.e., virus in the current study) removal effectiveness. Many existing literatures have investigated the impact of airflow pattern on ventilation efficiency relying either on CFD (Computational Fluid Dynamics) modelling [43,44] or experimental testing [45]. However, this is not a focus in this study. For simplicity, each sub-zone is assumed to be independent.

The ventilation control procedures are described as follows:

Step 1: Video acquisition of occupancy in each sub-zone (camera),

Step 2: Occupant detection using the bounding box of each frame using YOLO algorithm (microcontroller unit) (a microcontroller is a compact microcomputer designed for specific tasks in embedded systems, e.g., receiving sensor data, outputting signals),

Step 3: Occupant density calculation based on the bounding boxes of occupants and the boundary curves,

Step 4: Ventilation mode determination and rates calculation,

Step 5: Control signal transmission to the diffuser dampers (main and branch).

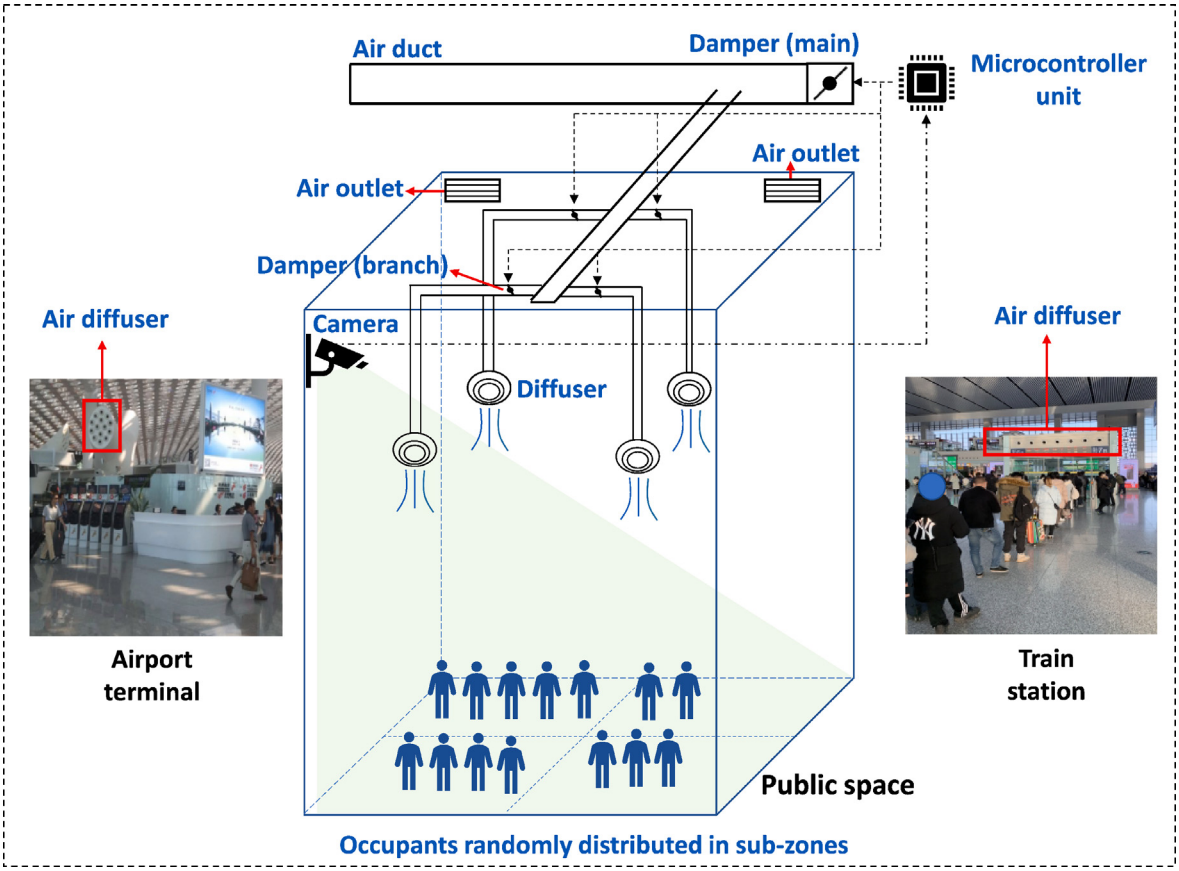

Fig. 5. Schematic diagram of the ventilation control in public transportation buildings.

2.3.2. Field studies

A lobby of a university building is selected to test the proposed camera-based occupant detection (shown in Fig. 6). The lobby area is 76.22 m^2 (with the length of 10.3 m and width of 7.4 m) with north and south corridors connected to the other rooms of the building. This lobby is the main entrance and exit for students and staffs. Thus, the occupancy scenarios are transient.

The lobby area is divided into four sub-zones corresponding to four ventilation air supply diffusers (numbered in Fig. 6(a)). The area of each sub-zone is 19 m^2 (76.22 m^2/4). To ensure a safe social distance of 2 m, each person is allowed to occupy a 1-m radius circle. In this application, by simply putting circles inside the area (each circle of 1-m radius), the maximum number of occupant density is 20 (see Fig. 6(b)). Therefore, each sub-zone can accommodate maximum 5 occupants to maintain a 2-m social distance. An occupant density of 0.26p/m^2 (5/19) is set as the threshold (i.e., "0") for each sub-zone.

A 2-megapixel surveillance camera with a 2.8 mm focal length was used to record the video. The video frame rate is 25 frames per second. Case 1 (13:50:00–13:58:00) is an 8-mins video which con-

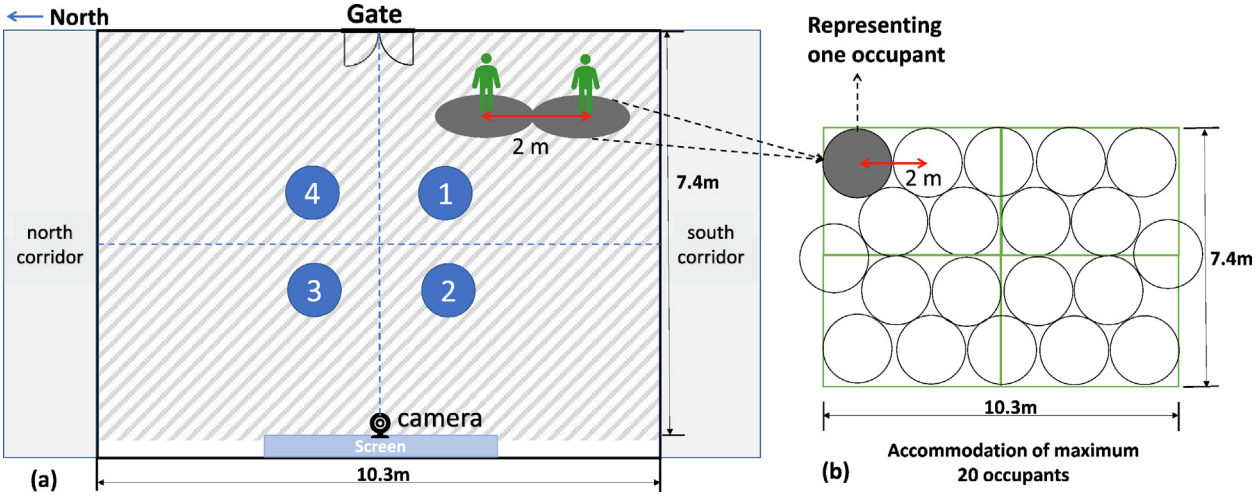

Fig. 6. (a) Lobby of the university building; (b) Illustration of occupants' accommodation.

tains dynamic occupant conditions and is used to validate the accuracy of occupant density detection. Case 2 (12:30:10–13:30:00) is a 1-hour video with various occupant scenarios and is used to demonstrate the IP and energy consumption of different ventilation strategies. A desktop computer is used to process the video, and the configuration is as follows: 6-core processor (AMD Ryzen 5 3600), 16 GB RAM (Random Access Memory), and NVIDIA GeForce GTX 1660 SUPER (graphics processing unit). The implementation of YOLO (v4) is based on [46], and the weights used can be found in [47].

2.3.3. Infection probability model

Wells-Riley model (equation (1)) is used for the infection risk evaluation and, the values of parameters are selected based on the following settings: P_d is set as 0.307 which is calculated by equation (2) with a distance (d) of 2 m; B is set as 2.2% based on the similar cases (Appendix B); q is the quantum generation rate and is selected as 0.238 quantum/s [15]; p is set as 8.2 L/min (or 1.37×10^{-4} m^3/h) based on the level of activities [48]; t is the time of exposure, which is estimated by common experience. For the airport terminal, the exposure time could be roughly 1 h or longer. For the train station, the typical exposure time is between 5mins to 1 h [48–50]. Here, the exposure time is set as 30mins.

2.4. Ventilation control strategies

In this study, the proposed ventilation mode, namely smart ventilation, is evaluated by the comparison with two other traditional ventilation control methods, i.e., fixed ventilation mode and DCV mode.

Strategy 1: fixed ventilation mode - fresh air ratio

This strategy fixes the fresh air supply ratio (defined as the outdoor airflow rate divided by the total air-conditioning supply air flow rate) at a certain value, e.g., 15%-30% [51]. Given a supply airflow rate, the fresh air flow rate is determined regardless of the occupancy condition.

Strategy 2: DCV mode - occupants' requirements

This strategy supplies the fresh air based on the demand which is quantified by occupant density. The ventilation rate for each occupant follows the recommended value in the design Standards (e.g., Table 1).

Strategy 3: smart ventilation mode - (proposed strategy)

In this strategy, the demand-controlled ventilation mode or anti-infection mode is used based on the threshold value (θ) of occupant density (Fig. 2). For the anti-infection mode, the ventilation rate will be determined by the targeted IP value using Wells-Riley model (see equation (1)).

3. Results

3.1. Validation of occupant density detection

A recorded video (Case 1) was used to validate the occupant density detection accuracy. The data sampling period was selected as 10 s to capture the occupancy dynamics. The regression functions of the horizontal and vertical boundary curves are shown in Fig. 7 (a) and (b). The quadratic functions were obtained through curve fitting and the R^2 (coefficient of determination) values of two boundary curves are 0.9734 and 0.9981, respectively.

48 continuous video frames were considered for validation. Specifically, this corresponded to 192 (48 frames $\times$ 4 sub-zones) data samples taken as the detected occupant densities for four different sub-zones, in which 26 detections are erroneous (86.5% data samples correct). The ground truth (true value, reflecting the real case) and the detected occupant density are shown in Fig. 8. Taking the sub-zone 1 as an example, the occupant density started from 0.21p/m^2, fluctuated and dropped to 0.05p/m^2, then raised up to 0.21p/m^2 again, and finally decreased to 0.05p/m^2. It can be clearly seen that the occupant densities experienced dynamic variations and were uneven in different sub-zones. By calculations, the average detection error of occupant density is 7.5% (or 92.5% of the accuracy), which is acceptable for engineering application. The detection error was calculated as: $\frac{|TV-DV|}{TV} \times 100\%$ ($TV$is the true value and DV is the detected value).

3.2. Analysis of infection probability (IP)

This section compares the ventilation rates and IP of three ventilation strategies, i.e., fixed ventilation, DCV and the proposed smart ventilation. Case 2 (see Section 2.3.2) was used for the evaluations of IP.

For the fixed ventilation (constant fresh air ratio of 15%), the ventilation rate is 101 m^3/h for each sub-zone (see Appendix A for the calculation details). For the DCV scenario, the sub-zonal ventilation rate ranges from 19 to 144 m^3/h, which varied linearly with the detected occupant density by three levels of ventilation rates (see Table 1). The smart ventilation targeted for a IP of 2% [15], and the ventilation rate is same with the DCV strategy when the sub-zone occupant density below the threshold (i.e., 0.26p/m^2); when the occupant density surpassed the threshold, the ventilation rate was set as "70·N" m^3/h (calculated based on equation (1)).

Fig. 9 shows that the IP of fixed ventilation rate was increased with the increasing occupant density. For the occupant density larger than 0.16p/m^2, the IP is out of the infection control target (i.e., 2%) and can reach up to 12.5% due to a constant but insufficient outdoor airflow rate. The IP of DCV is ranged from 2.9% to 8.5%, exceeding the targeted value of 2%. The main reason is that the primary goal of DCV is energy saving rather than infection prevention. On average, the DCV (an average IP of 6%) is slightly better than the fixed ventilation (an average IP of 6.5%) in terms of infection control. For the proposed smart ventilation, as the occupant density surpasses the safe threshold of 0.26p/m^2, the ventilation rate is increased immediately to prevent the transmission of infection, and to maintain the safe/targeted value of a 2% for IP. It is observed that the fixed or DCV ventilation strategies cannot reach the targeted lower value of IP in the majority of the situations, which agrees with a previous study [15]. Thus, improving the ventilation rate is generally recommended to reduce the risk of infection transmission in the public place.

3.3. Energy consumption of ventilation

Improving the ventilation rate is a simple and effective procedure in infection prevention, however the associated energy consumption cannot be neglected. Table 2 shows the energy consumption of three ventilation strategies for Case 2 (see Section 2.3.2). The COP of the air-conditioning system is set to be 4.2 [52]. The energy consumption of fixed ventilation is set as the benchmark. The strategy of DCV offers 66.6% of energy saving, but it cannot satisfy the goal of IP = 2% as mentioned before. The proposed smart ventilation strategy guarantees the IP goal of 2% in high occupancy conditions (namely the occupant density higher than 0.26p/m^2) and provides 11.7% of energy saving at the same time, which demonstrates a good potential to ensure both the energy efficiency and infection prevention.

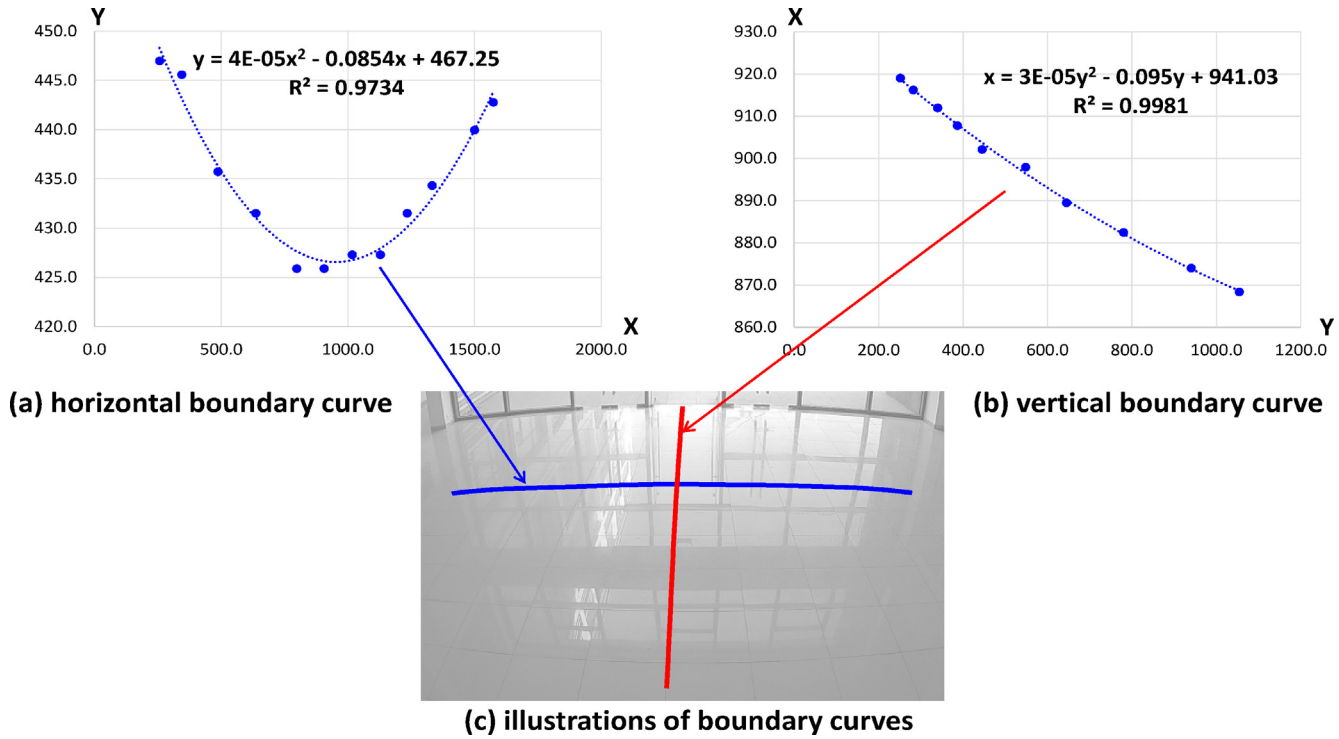

Fig. 7. The regression functions of boundary curves.

4. Demonstration of the hardware platform for occupant-based ventilation

4.1. The hardware platform and function realization

To realize the proposed smart ventilation system, a hardware prototype was constructed (shown in Fig. 10 (a)) based on a compact microcontroller (i.e., Raspberry Pi). Raspberry Pi can process different kinds of data and integrate cameras, sensors and other devices in one platform. The control process is as follow: acquiring video frame from the camera, data processing in Raspberry Pi, obtaining the occupant density and controlling the fan speed.

It should be noted that the implementation of the YOLO algorithm requires powerful computing unit. To estimate the occupant density in real-time with YOLO (i.e., 20 + frames per second), a NVIDIA Jetson NX (a powerful computing unit for video processing) or more powerful is required. Due to the limited hardware, this study uses the Raspberry Pi for demonstrating the idea of the proposed occupant-based ventilation control. Since the Raspberry Pi cannot implement YOLO in real-time, a more computationally friendly background substruction algorithm (i.e., Gaussian mixture model) was used in the demonstration. The Gaussian mixture model is a kind of background substruction algorithm and can extract the moving object as the foreground, with which the occupant density is estimated using the detected foreground pixels (details can be referred to [28]).

A test was conducted in a small conference room which covers an area of about 22 m^2 (3.4 m width and 6.5 m depth). The fan airflow rate was measured by an anemograph (the item 4 and 5 in Fig. 10). Fig. 11 shows that the fan speed can be effectively adjusted corresponding to different detected occupant density (i.e., occupant number). Although a 5-seconds delay was observed in the experiment due to the video processing time, this short delay is acceptable for practical application. The results demonstrate the feasibility of this hardware prototype in occupant-based ventilation control.

4.2. Alerting system (e.g., email)

Based on the above-mentioned Raspberry Pi platform, an alert system can be integrated. A Python code (Fig. 12) was developed to send an email to alert the building manager or corresponding persons when the occupancy threshold is violated in any sub-zones of the public space. This function enables the automatic monitoring based on the real-time occupant detection, which could liberate some manpower from monitoring and thus improve the entire building management efficiency in PPBs. The released manpower can be put into more critical and emergent tasks.

5. Discussions for the benefits of proposed ventilation control strategy

5.1. Identifications of sub-zone infection risks

An advantage of the proposed camera-based occupant detection method is that the sub-zone occupant density can be detected and the associated risk could be calculated. Without the sub-zone occupant information, only an overall occupant density can be observed, i.e., 8/76.22 = 0.105p/m^2 for the case shown in Fig. 13. With the proposed occupant detection, the occupant density of the sub-zone can be computed, i.e., 8/19 = 0.421p/m^2 which is higher than the threshold value of 0.26p/m^2. Actions, like increasing the ventilation rate and broadcasting alerts, can be taken immediately to reduce the occupant density so as the infection transmission risk.

5.2. Ventilation for infection prevention-a proactive measure from engineering perspective

Wearing masks and keeping social distance are certainly two effective measures to lower down the infection risk of COVID-19 [12]. However, these two measures are controlled subjectively, which is not “robust”. Any individual carrying with the coronavirus

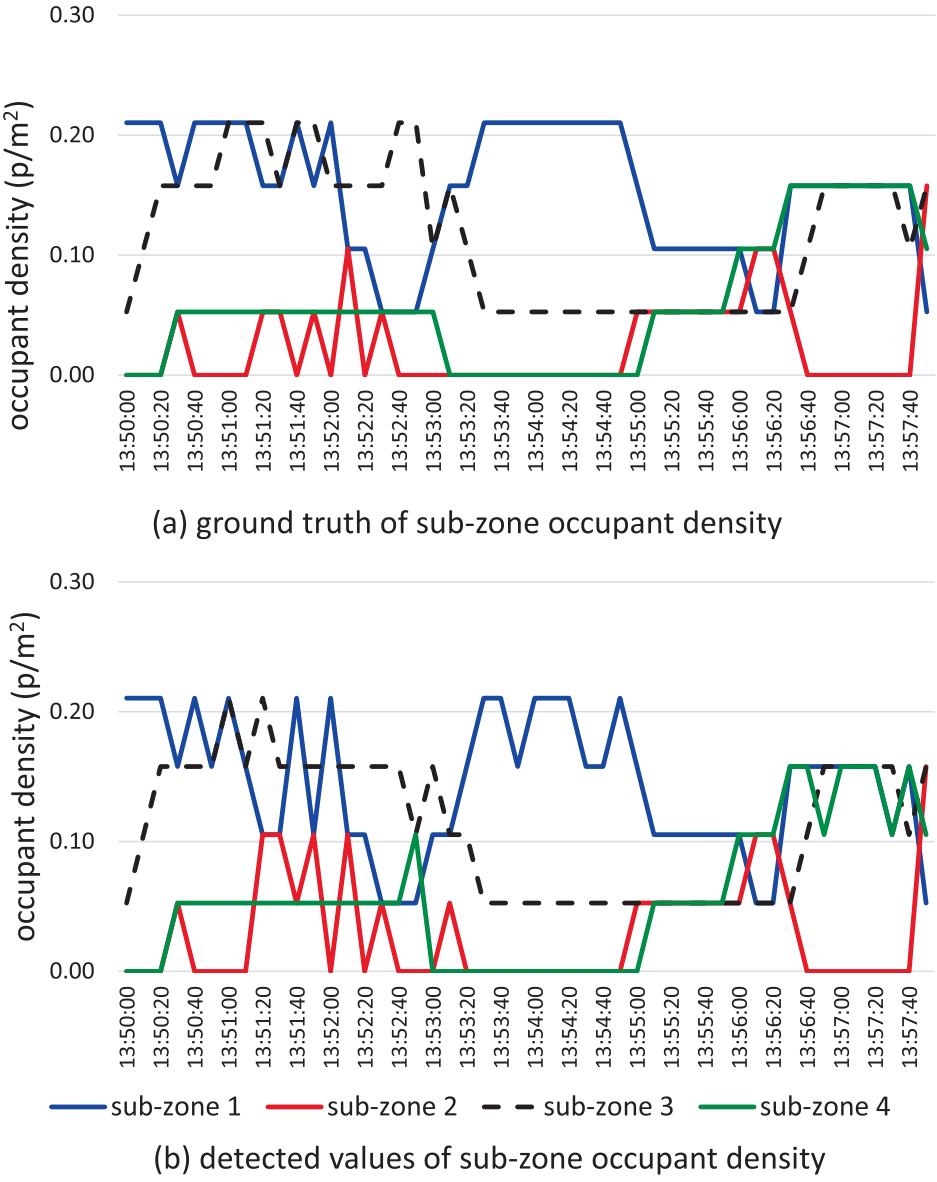

Fig. 8. Sub-zone occupant density: (a) ground truth and (b) detected values.

that does not stick to the mandatory rules would cause a potential infection risk. Besides, occupants may remove face masks (drinking or eating) and stay close (talking) occasionally in public space. Thus, relying solely on personal subjective behaviors is not robust to prevent occupant from being infected. In such scenario, the ventilation rate can be adjusted based on occupant density and behavior information to reduce the risk of infection. This is an effective and efficient approach.

5.3. Solution for improving ventilation efficiency from the perspectives of saving energy and mitigating infection risk

How to balance the ventilation energy consumption and reduce the infection probability risk in PPBs is a critical issue in the current society. The proposed smart ventilation strategy was compared with two other traditional ventilation modes, namely fixed ventilation (using a fixed fresh air ratio), demand-controlled ventilation (DCV based on occupant density). Given a targeted IP value of 2%, the fixed ventilation mode normally consumes more energy, e.g., higher ventilation rates supplied during lower occupant density. From infection control point of view, this fixed mode provides inadequate ventilation for the case of dense occupancy (which results in an IP of 12.5%). The DCV is an improved ventilation mode which adjusted ventilation rates based on occupant density, which leads to a 66.6% of energy saving (compared with the fix ventilation mode). The IP in such a scenario can be reached up to 8.5% (4% lower than the fixed ventilation mode). The proposed smart ventilation strategy considers both energy conservation (required ventilation rates from occupant density detection) as well as infection risk control. This strategy can lower the IP value to 2%, while reaching 11.7% of energy saving compared with the fixed ventilation mode. The advantage of the proposed strategy is that the DCV mode and the anti-infection mode can be switched based on the occupancy situation and infection risk calculation (Wells-Riley model). The proposed ventilation strategy provides a smart solution for tackling the above dilemma considering both energy efficiency and infection risk.

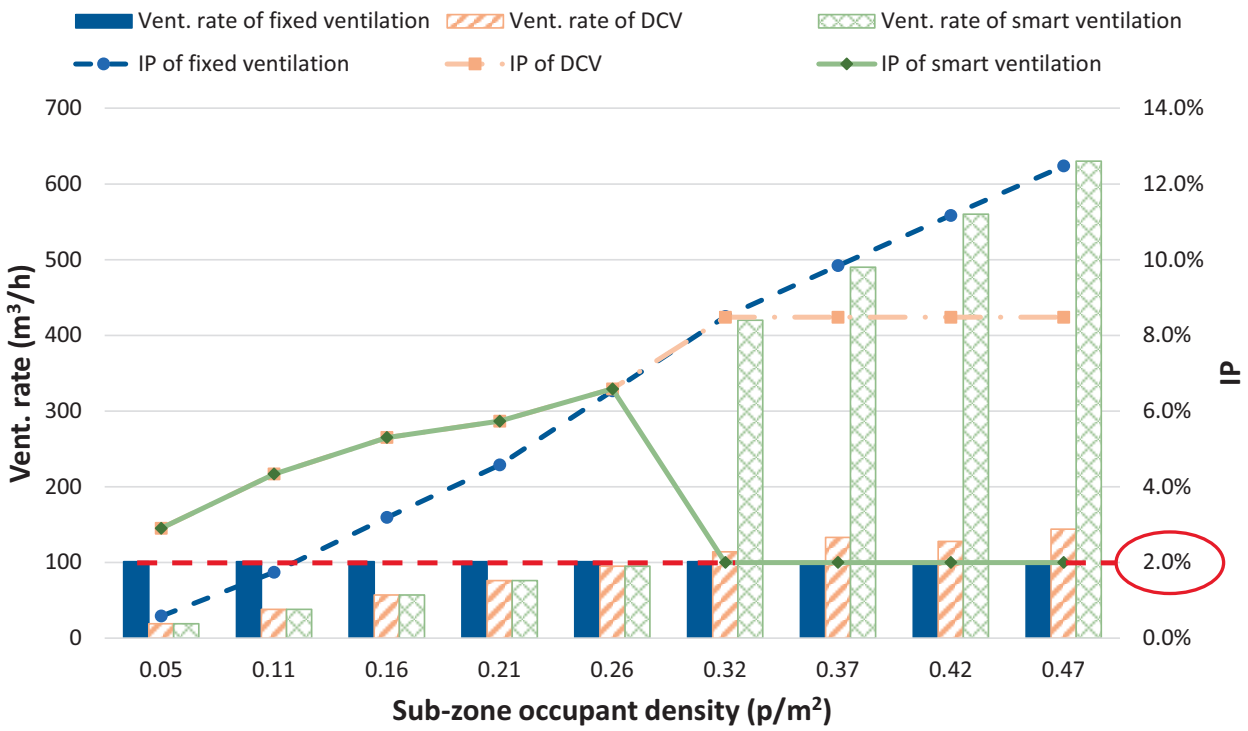

Fig. 9. Ventilation rate and IP of three ventilation strategies ("Vent." represents ventilation).

Table 2
Energy consumption of ventilation.

Ventilation strategy	Energy consumption (Wh)	Energy saving ratio (%)
Fixed ventilation	2911.7	/
DCV	973.7	66.6%
Smart ventilation	2570.5	11.7%

5.4. Practical implications

To realize and apply the proposed smart ventilation in this study, a microcontroller-based hardware prototype has been developed and tested. Besides, an email alert system is integrated to inform the occupants in real time in order to reduce the risk of infection transmission. The developed hardware prototype can be readily applied in PPBs and many other building spaces with a relatively low cost (the microcontroller costs around US $60). Besides, the automatic and real-time detection of occupant density can release the manpower for more critical tasks, bring extended value. Currently, mutations in SARS-CoV-2 have been observed, which may reduce the effect of vaccine and can cause another wave of epidemic [53]. In the next few years, the epidemic prevention and control probably may become the regular routine in public spaces. Constructing a healthy yet sustainable society is a urgent need now [54]. The developed hardware prototype of the smart ventilation is especially meaningful under the long-term risk of COVID-19 (or alike diseases), which can be a feasible and promising solution to build healthy yet sustainable indoor environments for public buildings.

5.5. Limitations

In our work, we focused on the high-dense building environment which may have potentially high risk of infection transmission. The ideal way to determine the ventilation rate is based on the concentration of virus and the location of the infected person (s). Unfortunately, the virus or infected person is difficult to be either detected or monitored. Therefore, the occupant-density-detection based ventilation system is proposed and a modified Wells-Riley model was used to evaluate the infection risk, based on which the ventilation rate was estimated. The main limitation of the camera-based occupant detection is that the occlusion of the video frame due to dense occupants, could miss the detection. A possible solution is to place the camera on the ceiling to minimize the occlusion.

In the Wells-Riley model, the parameter B (initial infection rate) is estimated based on the reported infection cases, while the q (quantum generation rate) is referred to a similar study [15]. However, the values of parameters in the Wells-Riley model are case-dependent (e.g., an infected person may have a higher quantum generation rate than the assumed one). Given that the ventilated rate calculated from the Wells-Riley model is a minimal value, the ventilation rate can be further increased in practice to secure a lower IP and compensate the uncertainties of the assumed parameter values.

The calculated ventilation rates for infection prevention (maximum 630 m^3/h) are all below the design rate of supply air (709 m^3/h). Thus, it is achievable in the presented case study. However, in some cases of high-dense occupancy, the calculated ventilation rate may not be achieved by the existing ventilation system. Some assistance measures can be used to loosen the existing ventilation system requirement. For instance, the alert system (presented in Section 4) could be used to control the occupant density by redirecting the crowd moment. Some social distance tapes can also be put into practice to enhance the social distancing. With a relatively lower occupant density, the required minimal ventilation rate can be reduced.

Further control measures such as the installation of the filtration module and the UV (ultraviolet) lighting module can reduce the risk of spreading virus. For the sake of practical applications, this study simplifies the situations and assumed independency of ventilation among sub-zones. In reality, sub-zones would interact

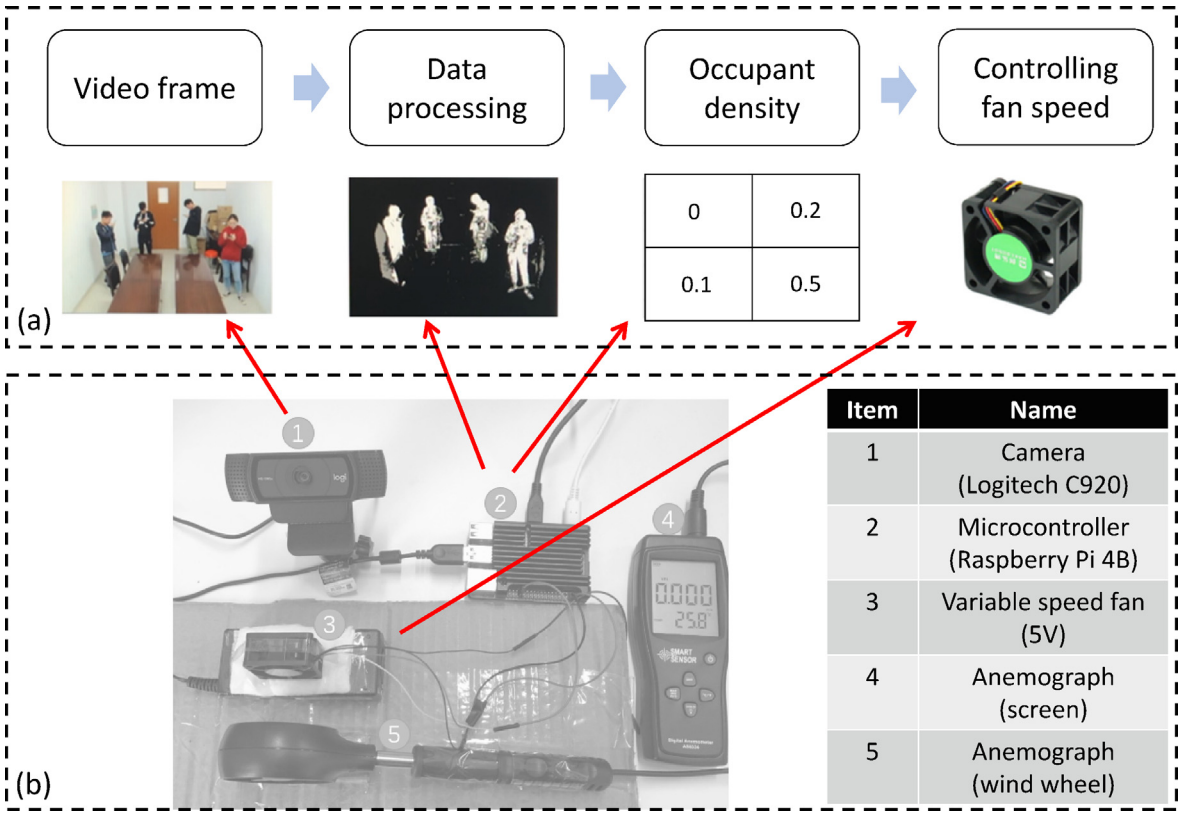

Fig. 10. (a) the control schematic; (b) hardware prototype

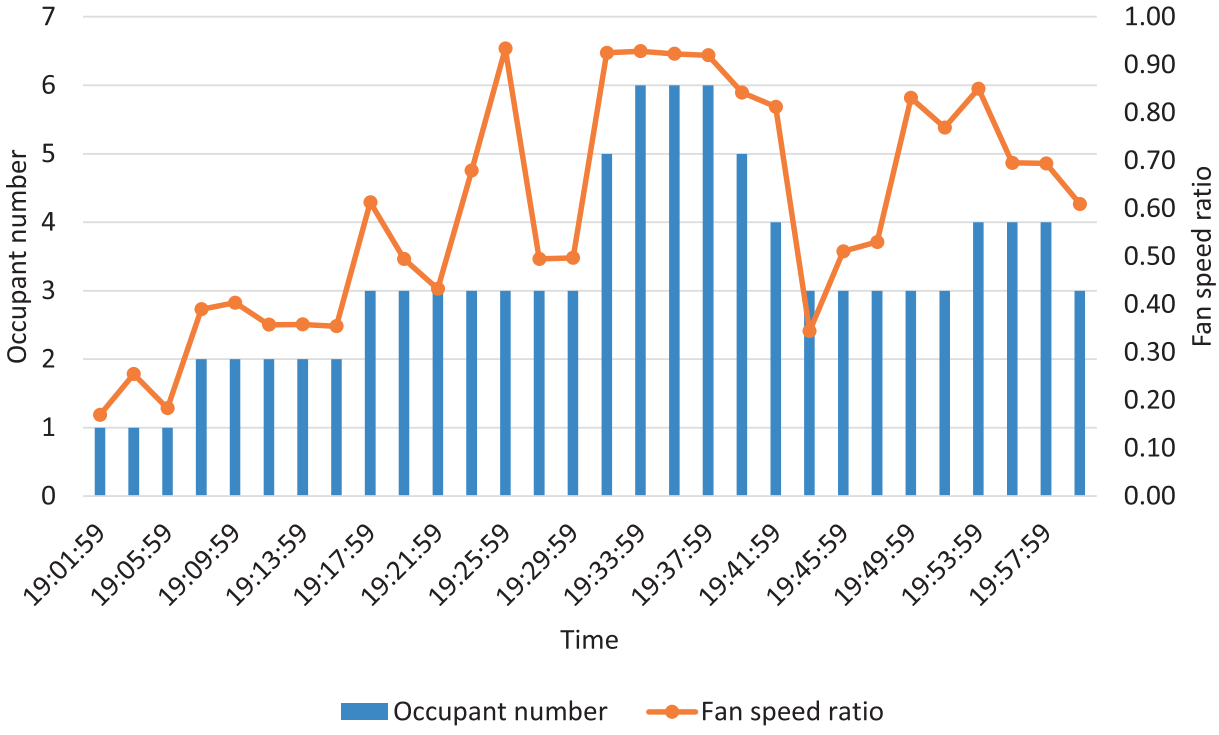

Fig. 11. Occupant number and fan speed ratio.

with each other. Future studies can be planned to investigate the cross infections and interactions of multiple diffusers on the targeted zone.

6. Conclusions

This paper proposes a smart ventilation control that can actively self-adjust the ventilation rate when experiencing differ-

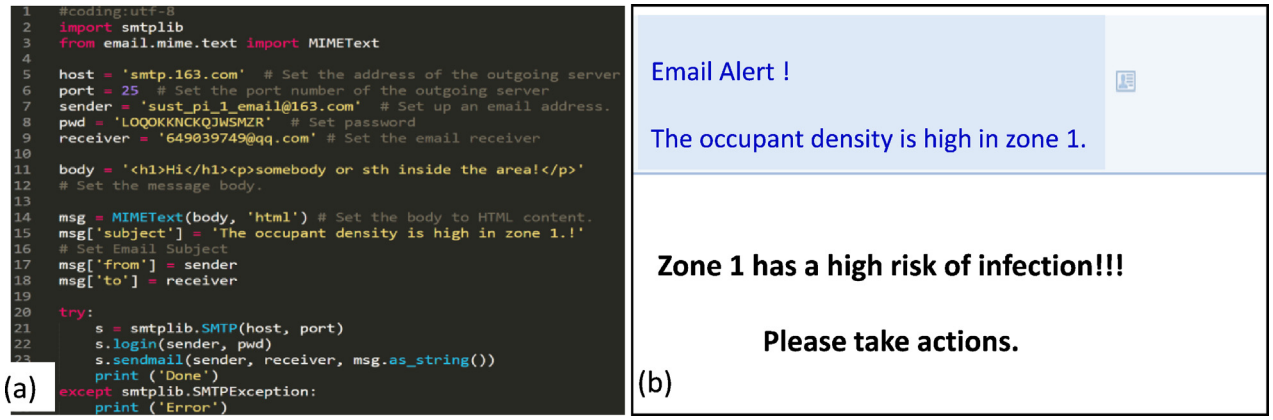

Fig. 12. Email alert based on Raspberry Pi: (a) Python code (b) email example.

Fig. 13. A case of crowd gathering in a sub-zone.

ent occupant densities, with objectives of both mitigating infection risk of long-distance aerosol transmission and saving ventilation energy. The main conclusions are summarized below.

(1) The YOLO-based occupant detection algorithms achieved a 92.5% of the detection accuracy, which is acceptable for practical application.
(2) The proposed smart ventilation strategy can lower the infection probability and save energy consumption when compared with the traditional fixed ventilation mode. For the current study, with 15% outdoor air ratio as a test case, the infection probability can be up to 12.5%; the proposed ventilation mode can lower infection probability to 2% and save 11.7% of energy consumption.
(3) A low-cost microcontroller-based hardware prototype is developed to realize both functions of occupant density detection and ventilation control.

It should be noted that ventilation is one of the important prevention measures. Wearing masks, keeping social distancing and well-maintained hygiene are important ways that personnel can contribute, which will continually be recommended or reinforced in the future. However, with the chances of off-mask activities, close contact and insanitation, the ventilation control becomes essential as a proactive prevention measure in public spaces. Besides, given the rapid evaporation process (0.17 s and 0.4 s) of small droplets to droplet nuclei [55], a real-time occupant-density-detection based ventilation control would be extremely important.

Declaration of Competing Interest

The authors declare that they have no known competing financial interests or personal relationships that could have appeared to influence the work reported in this paper.

Acknowledgement

The authors would like to acknowledge the supports from Natural Science Foundation of China (Grand No. 51778385), Natural Science Foundation of Jiangsu Province of China (Grand No. BK20190942), and Innovation and Entrepreneurship Talents Introduction Program of Jiangsu Province of China (Grand No. 492011302).

Table B1
Data of reported infection cases.

Cases	Number of initial infector(s)	Number of final infections	Number of people	Initial infection rate
Bus in Hunan, China	1	8	48	2.1%
Airflight	3	7	86	3.5%
Bus in Ningbo, China	1	25	68	1.5%
Airplane in Iran	5	37	311	1.61%

Table A1
The calculation of heating load in the case study.

Envelop items	area (m^2)	heat conduction coefficient (W/m·K)	Δtbetween indoor and outdoor (°C)	CF forΔt	basic heat loss (W)	CF for heat loss	corrected heat loss (W)	heating load (W)
north internal wall	22.2	1.72	20.5	0.6	469.7	1	469.7	469.7
south internal wall	22.2	1.72	20.5	0.6	469.7	1	469.7	469.7
east glass façade	30.9	2.5	20.5	1	1583.6	0.95	1504.4	1504.4
west internal wall	30.9	1.72	20.5	0.6	653.7	1	653.7	653.7
ceiling	76.22	0.77	20.5	0.6	721.9	1	721.9	721.9
ground	76.22	0.77	20.5	1	1203.1	1	1203.1	1203.1
								5022.5

(Δt is temperature difference; CF stands for correction factor. The heat conduction coefficients and CF values can refer to [6].)

Appendix A. . Calculation of ventilation load for the case study

The case study was conducted in the Winter. Thus, the heating load was calculated. The design settings are presented as follows: supply air temperature is 24 °C, room air temperature is 18 °C, specific heat of air is 1.005 kJ/(kg·°C), density of air is 1.17 kg/m^3, and ambient outdoor air temperature is −2.5 °C for air-conditioning at the design condition of Suzhou, China. From Table A1, the heating load is 5022.5 W.

Appendix B. . Parameters of the reported infection cases

Based on the cases reported in Table B1, the average initial infection rate (i.e., 2.2%) is used in the calculation of IP.

Appendix C. . MATLAB code - obtain the pixel coordinates (x, y)

```
im_read_current_cell = imread('C:\Users\Desktop\1.jpg'); (input file location in brackets)
imshow(im_read_current_cell);
[x_screen,y_screen] = ginput;
```

References

[1] C. Xu, X. Luo, C. Yu, S.-J. Cao, The 2019-nCoV epidemic control strategies and future challenges of building healthy smart cities, Indoor Built Environ. 29 (5) (2020) 639–644, https://doi.org/10.1177/1420326X20910408.

[2] Z. Noorimotlagh, N. Jaafarzadeh, S.S. Martínez, S.A. Mirzaee, A systematic review of possible airborne transmission of the COVID-19 virus (SARS-CoV-2) in the indoor air environment, Environ. Res. 193 (2021) 110612, https://doi.org/10.1016/j.envres.2020.110612.

[3] WHO, Coronavirus Disease (COVID-19) Dashboard, (2021). https://covid19.who.int/.

[4] J. Wang, Vision of China's future urban construction reform: In the perspective of comprehensive prevention and control for multi disasters Sustain, Cities Soc. 64 (2021) 102511, https://doi.org/10.1016/j.scs.2020.102511.

[5] ASHRAE, ANSI/ASHRAE standrad 62.1-2019, (2019).

[6] GB-50736, Design code for heating ventilation and air conditioning of civil buildings, China Building Industry Press, Beijing, 2012.

[7] J. Ding, C.W. Yu, S.-J. Cao, HVAC systems for environmental control to minimize the COVID-19 infection, Indoor Built Environ. 29 (9) (2020) 1195–1201, https://doi.org/10.1177/1420326X20951968.

[8] V. Antony Aroul Raj, R. Velraj, F. Haghighat, The contribution of dry indoor built environment on the spread of Coronavirus: Data from various Indian states, Sustain. Cities Soc. 62 (2020) 102371, https://doi.org/10.1016/j.scs.2020.102371.

[9] N. van Doremalen, T. Bushmaker, D.H. Morris, M.G. Holbrook, A. Gamble, B.N. Williamson, A. Tamin, J.L. Harcourt, N.J. Thornburg, S.I. Gerber, J.O. Lloyd-Smith, E. de Wit, V.J. Munster, Aerosol and Surface Stability of SARS-CoV-2 as Compared with SARS-CoV-1, New Engl. J. of Med. 382 (16) (2020) 1564–1567, https://doi.org/10.1056/NEJMc2004973.

[10] A.W.H. Chin, J.T.S. Chu, M.R.A. Perera, K.P.Y. Hui, H.-L. Yen, M.C.W. Chan, M. Peiris, L.L.M. Poon, Stability of SARS-CoV-2 in different environmental conditions, The Lancet Microbe. 1 (1) (2020) e10, https://doi.org/10.1016/S2666-5247(20)30003-3.

[11] L.J. Schoen, Guidance for building operations during the COVID-19 pandemic, ASHRAE J. 62 (2020) 72–74.

[12] D.K. Chu, E.A. Akl, S. Duda, K. Solo, S. Yaacoub, H.J. Schünemann, D.K. Chu, E.A. Akl, A. El-harakeh, A. Bognanni, T. Lotfi, M. Loeb, A. Hajizadeh, A. Bak, A. Izcovich, C.A. Cuello-Garcia, C. Chen, D.J. Harris, E. Borowiack, F. Chamseddine, F. Schünemann, G.P. Morgano, G.E.U. Muti Schünemann, G. Chen, H. Zhao, I. Neumann, J. Chan, J. Khabsa, L. Hneiny, L. Harrison, M. Smith, N. Rizk, P. Giorgi Rossi, P. AbiHanna, R. El-khoury, R. Stalteri, T. Baldeh, T. Piggott, Y. Zhang, Z. Saad, A. Khamis, M. Reinap, S. Duda, K. Solo, S. Yaacoub, H.J. Schünemann, Physical distancing, face masks, and eye protection to prevent person-to-person transmission of SARS-CoV-2 and COVID-19: a systematic review and meta-analysis, Lancet. 395 (10242) (2020) 1973–1987, https://doi.org/10.1016/S0140-6736(20)31142-9.

[13] News BBC, Coronavirus: US airports in disarray over screening, (2020). https://www.bbc.com/news/world-us-canada-51895246.

[14] W. Bendibao https://www.sohu.com/a/278269878_693076.

[15] C. Sun, Z. Zhai, The efficacy of social distance and ventilation effectiveness in preventing COVID-19 transmission, Sustain. Cities Soc. 62 (2020) 102390, https://doi.org/10.1016/j.scs.2020.102390.

[16] T. Abuimara, W. O'Brien, B. Gunay, Quantifying the impact of occupants' spatial distributions on office buildings energy and comfort performance, Energy Build. 233 (2021) 110695, https://doi.org/10.1016/j.enbuild.2020.110695.

[17] B. Merema, M. Delwati, M. Sourbron, H. Breesch, Demand controlled ventilation (DCV) in school and office buildings: Lessons learnt from case studies, Energy Build. 172 (2018) 349–360, https://doi.org/10.1016/j.enbuild.2018.04.065.

[18] F. Haghighat, G. Donnini, Conventional vs CO2 demand-controlled ventilation systems, J. Therm. Biol. 18 (5-6) (1993) 519–522, https://doi.org/10.1016/0306-4565(93)90085-8.

[19] C. Ren, S.-J. Cao, Development and application of linear ventilation and temperature models for indoor environmental prediction and HVAC systems control, Sustain. Cities Soc. 51 (2019) 101673, https://doi.org/10.1016/j.scs.2019.101673.

[20] C. Ren, S.-J. Cao, Implementation and visualization of artificial intelligent ventilation control system using fast prediction models and limited monitoring data, Sustain. Cities Soc. 52 (2020) 101860, https://doi.org/10.1016/j.scs.2019.101860.

[21] H.-C. Zhu, C.W. Yu, S.-J. Cao, Ventilation online monitoring and control system from the perspectives of technology application, Indoor Built Environ. 29 (4) (2020) 587–602, https://doi.org/10.1177/1420326X19878586.
[22] Z. Pang, Y. Chen, J. Zhang, Z. O'Neill, H. Cheng, B. Dong, Nationwide HVAC energy-saving potential quantification for office buildings with occupant-centric controls in various climates, Appl. Energy. 279 (2020) 115727, https://doi.org/10.1016/j.apenergy.2020.115727.
[23] M. Jin, N. Bekiaris-Liberis, K. Weekly, C.J. Spanos, A.M. Bayen, Occupancy Detection via Environmental Sensing, IEEE Trans. Autom. Sci. Eng. 15 (2) (2018) 443–455, https://doi.org/10.1109/TASE.2016.2619720.
[24] J. Wang, N.C.F. Tse, J.Y.C. Chan, Wi-Fi based occupancy detection in a complex indoor space under discontinuous wireless communication: A robust filtering based on event-triggered updating, Build. Environ. 151 (2019) 228–239, https://doi.org/10.1016/j.buildenv.2019.01.043.
[25] W. Wang, J. Wang, J. Chen, G. Huang, X. Guo, Multi-zone outdoor air coordination through Wi-Fi probe-based occupancy sensing, Energy Build. 159 (2018) 495–507, https://doi.org/10.1016/j.enbuild.2017.11.041.
[26] J.P. Roselyn, R.A. Uthra, A. Raj, D. Devaraj, P. Bharadwaj, S.V.D. Krishna Kaki, Development and implementation of novel sensor fusion algorithm for occupancy detection and automation in energy efficient buildings, Sustain. Cities Soc. 44 (2019) 85–98, https://doi.org/10.1016/j.scs.2018.09.031.
[27] J. Zou, Q. Zhao, W. Yang, F. Wang, Occupancy Detection in the Office by Analyzing Surveillance Videos and its Application to Building Energy Conservation, Energy Build. 152 (2017) 385–398.
[28] J. Wang, N. Tse, T. Poon, J. Chan, A practical multi-sensor cooling demand estimation approach based on visual, indoor and outdoor information sensing, Sensors (Switzerland). 18 (11) (2018) 3591, https://doi.org/10.3390/s18113591.
[29] M. Shorfuzzaman, M.S. Hossain, M.F. Alhamid, Towards the sustainable development of smart cities through mass video surveillance: A response to the COVID-19 pandemic, Sustain. Cities Soc. 64 (2021) 102582, https://doi.org/10.1016/j.scs.2020.102582.
[30] I. Ahmed, M. Ahmad, J.J.P.C. Rodrigues, G. Jeon, S. Din, A deep learning-based social distance monitoring framework for COVID-19, Sustain. Cities Soc. 65 (2021) 102571, https://doi.org/10.1016/j.scs.2020.102571.
[31] P. Nagrath, R. Jain, A. Madan, R. Arora, P. Kataria, J. Hemanth, SSDMNV2: A Real time DNN-Based Face Mask Detection System using Single Shot Multibox Detector and MobileNetV2, Sustain. Cities Soc. 66 (2021) 102692, https://doi.org/10.1016/j.scs.2020.102692.
[32] M. Loey, G. Manogaran, M.H.N. Taha, N.E.M. Khalifa, Fighting against COVID-19: A novel deep learning model based on YOLO-v2 with ResNet-50 for medical face mask detection, Sustain. Cities Soc. 65 (2021) 102600, https://doi.org/10.1016/j.scs.2020.102600.
[33] Y.u. Feng, T. Marchal, T. Sperry, H. Yi, Influence of wind and relative humidity on the social distancing effectiveness to prevent COVID-19 airborne transmission: A numerical study, J. Aerosol Sci. 147 (2020) 105585, https://doi.org/10.1016/j.jaerosci.2020.105585.
[34] L. Setti, F. Passarini, G. De Gennaro, P. Barbieri, M.G. Perrone, M. Borelli, J. Palmisani, A. Di Gilio, P. Piscitelli, A. Miani, Airborne transmission route of covid-19: Why 2 meters/6 feet of inter-personal distance could not be enough, Int. J. Environ. Res. Public Health. 17 (8) (2020) 2932, https://doi.org/10.3390/ijerph17082932.
[35] Y. Guo, H. Qian, Z. Sun, J. Cao, F. Liu, X. Luo, R. Ling, L.B. Weschler, J. Mo, Y. Zhang, Assessing and controlling infection risk with Wells-Riley model and spatial flow impact factor (SFIF), Sustain. Cities Soc. 67 (2021) 102719, https://doi.org/10.1016/J.SCS.2021.102719.
[36] E.C. Riley, G. Murphy, R.L. Riley, Airborne spread of measles in a suburban elementary school, Am. J. Epidemiol. 107 (1978) 421–432, https://doi.org/10.1093/oxfordjournals.aje.a112560.
[37] Redmon J., Divvala S., Girshick R., Farhadi A. You Only Look Once: Unified, Real-Time Object Detection, in: IEEE Conf. Comput. Vis. Pattern Recognit., Las Vegas, NV, USA, 2016: pp. 779–788.
[38] Hendry, R.-C. Chen, Chen, Automatic License Plate Recognition via sliding-window darknet-YOLO deep learning, Image Vis. Comput. 87 (2019) 47–56, https://doi.org/10.1016/j.imavis.2019.04.007.
[39] Z. Cao, T. Liao, W. Song, Z. Chen, C. Li, Detecting the shuttlecock for a badminton robot: A YOLO based approach, Expert Syst. Appl. 164 (2021) 113833, https://doi.org/10.1016/j.eswa.2020.113833.
[40] P.u. Li, W. Zhao, Image fire detection algorithms based on convolutional neural networks, Case Stud. Therm. Eng. 19 (2020) 100625, https://doi.org/10.1016/j.csite.2020.100625.
[41] A. Bochkovskiy, C.Y. Wang, H.Y.M. Liao, YOLOv4: Optimal Speed and Accuracy of Object Detection, ArXiv. (2020).
[42] ASHRAE, ASHRAE Handbook-Fundamentals, American Society of Heating, Refrigerating and Air-Conditioning Engineers (2017).
[43] S.J. Cao, C. Ren, Ventilation control strategy using low-dimensional linear ventilation models and artificial neural network, Build. Environ. 144 (2018) 316–333, https://doi.org/10.1016/j.buildenv.2018.08.032.
[44] G. Cao, H. Awbi, R. Yao, Y. Fan, K. Sirén, R. Kosonen, J. (Jensen) Zhang, A review of the performance of different ventilation and airflow distribution systems in buildings, Build. Environ. 73 (2014) 171–186, https://doi.org/10.1016/j.buildenv.2013.12.009.
[45] H.Y. Deng, Z. Feng, S.J. Cao, Influence of air change rates on indoor CO2 stratification in terms of Richardson number and vorticity, Build. Environ. 129 (2018) 74–84, https://doi.org/10.1016/j.buildenv.2017.12.009.
[46] Y. Chen, Object-Detection-and-Tracking https://github.com/yehengchen/Object-Detection-and-Tracking/tree/master/OneStage/yolo/deep_sort_yolov4.
[47] A. Bochkovskiy, darknet https://github.com/AlexeyAB/darknet%0A.
[48] X. Duan, X. Zhao, B. Wang, Exposure factors handbook of Chinese population, China Environmental Science Press, Beijing, 2013.
[49] J.B. Ingvardson, O.A. Nielsen, S. Raveau, B.F. Nielsen, Passenger arrival and waiting time distributions dependent on train service frequency and station characteristics: A smart card data analysis, Transp. Res. Part C Emerg. Technol. 90 (2018) 292–306, https://doi.org/10.1016/j.trc.2018.03.006.
[50] Y. Fan, A. Guthrie, D. Levinson, Waiting time perceptions at transit stops and stations: Effects of basic amenities, gender, and security, Transp. Res. Part A Policy Pract. 88 (2016) 251–264, https://doi.org/10.1016/j.tra.2016.04.012.
[51] Y. Cheng, S. Zhang, C. Huan, M.O. Oladokun, Z. Lin, Optimization on fresh outdoor air ratio of air conditioning system with stratum ventilation for both targeted indoor air quality and maximal energy saving, Build. Environ. 147 (2019) 11–22, https://doi.org/10.1016/j.buildenv.2018.10.009.
[52] GB50189, Design standard for energy efficiency of public buildings, (2015).
[53] B. Korber, W.M. Fischer, S. Gnanakaran, H. Yoon, J. Theiler, W. Abfalterer, N. Hengartner, E.E. Giorgi, T. Bhattacharya, B. Foley, K.M. Hastie, M.D. Parker, D.G. Partridge, C.M. Evans, T.M. Freeman, T.I. de Silva, C. McDanal, L.G. Perez, H. Tang, A. Moon-Walker, S.P. Whelan, C.C. LaBranche, E.O. Saphire, D.C. Montefiori, A. Angyal, R.L. Brown, L. Carrilero, L.R. Green, D.C. Groves, K.J. Johnson, A.J. Keeley, B.B. Lindsey, P.J. Parsons, M. Raza, S. Rowland-Jones, N. Smith, R.M. Tucker, D. Wang, M.D. Wyles, Tracking Changes in SARS-CoV-2 Spike: Evidence that D614G Increases Infectivity of the COVID-19 Virus, Cell. 182 (4) (2020) 812–827.e19, https://doi.org/10.1016/j.cell.2020.06.043.
[54] N.A. Megahed, E.M. Ghoneim, Antivirus-built environment: Lessons learned from Covid-19 pandemic, Sustain. Cities Soc. 61 (2020) 102350, https://doi.org/10.1016/j.scs.2020.102350.
[55] M. Nicas, W.W. Nazaroff, A. Hubbard, Toward understanding the risk of secondary airborne infection: Emission of respirable pathogens, J. Occup. Environ. Hyg. 2 (3) (2005) 143–154, https://doi.org/10.1080/15459620590918466.